Optics Communications 281 (2008) 4268–4272

Contents lists available at ScienceDirect

Optics Communications

journal homepage: www.elsevier.com/locate/optcom

Application of interference microscopy to the study of hologram build-up in $LiNbO_3$ crystals

István Bányász *, Gábor Mandula

Department of Crystal Physics, Research Institute of Solid State Physics and Optics of the Hungarian Academy of Sciences, P.O. Box 49, H-1525 Budapest, Hungary

ARTICLE INFO

Article history:
Received 26 November 2007
Received in revised form 31 March 2008
Accepted 22 April 2008

PACS:
42.40
42.40Kw
42.65Hw
42.70Nq
07.60Pb

Keywords:
Photorefractive crystals
Lithium niobate
Holography
Interference microscopy

ABSTRACT

Interference microscopy was applied to direct microscopic observation of temporal evolution of phase holograms in $LiNbO_3$:Fe photorefractive crystals. First a hologram was recorded in the sample, and diffraction efficiency was monitored during hologram build-up using inactinic laser light. Thus kinetics of hologram build-up could be determined. The initial hologram was erased using white light. Then a series of write-erase cycles were performed with increasing exposure times. Holograms were observed by interference microscope after each exposure. The time elapsed between the exposure and the microscopic observation was negligible compared to the relaxation time of the hologram. The obtained temporal evolution of the grating profile gives a deeper insight into the physical mechanism of hologram formation in photorefractive materials than simple diffraction efficiency measurements. A congruently grown sample of $LiNbO_3$ doped with 10^{-3} mol/mol Fe in melting was studied by this method. Sample thickness was set to 300 μm to allow correct microscopic observation. Plane-wave holograms were recorded in the samples using an Ar–ion laser at $\lambda = 488.0$ nm of grating constants of 3, 6.5 and 8.8 μm.

1. Introduction

Since its discovery in 1966, the photorefractive effect has been studied extensively by several methods in various materials and has turned out to play a key role in modern optical technologies like photonics [1]. The holograms or simple gratings created by the effect have been experimentally studied mainly by measuring its diffraction efficiency or by reconstructing the recorded hologram. Relatively few papers report microscopic investigation of photorefractive gratings. In 1988, Matull and Rupp investigated thermally fixed holograms in copper doped lithium niobate crystals by microphotometric method, and measured not only the intensity but also the phase distribution of the light intensity pattern at the exit face of the crystal [2,3]. Brody and Garvin [4] developed a real-time laser holographic microscope using a photorefractive hologram and digital signal processing in 1990. Poumellec et al. [5] reported an ultraviolet light induced densification during Bragg grating inscription in $Ge:SiO_2$ using interferometric microscopy in 1995. In the following year, Grabar et al. published their three-dimensional investigation of domain structures of uniaxial ferroelectrics by applying photorefractive grating and polarization microscope [6]. In 1997, Douay et al. reported the monitoring of the build-up of photorefractive grating in PZG glass thin film both by He–Ne laser and interferometric microscope [7]. By using both optical and scanning electron microscope, Cipparrone et al. showed that the basic mechanism of the optical storage effect in dye-doped polymer dispersed liquid crystals is the photorefractive effect [8]. Atomic force microscopy was used for the direct study of charge grating at the surface of $LiNbO_3$ crystal by Soergel et al. [9]. Zhao et al. studied waveguide structures recorded in $LiNbO_3$:Fe, KNSBN:Ce and SBN:Cr crystals using digital holography with a Mach-Zehnder interferometer and a CCD camera [10]. de Angelis et al. adapted digital holography to the study of static holographic gratings recorded in iron doped lithium niobate [11].

However, no work on microscopic study of the build-up of two-wave mixing volume gratings of high spatial frequency in a photorefractive crystal has been reported so far. In the present article we report a quasi in-situ investigation of the build-up of photorefractive gratings in $LiNbO_3$:Fe.

Systematic study of phase gratings fabricated via ion-implantation in glass both with interference- and phase-contrast microscopy was performed by one of the authors of the present article

* Corresponding author. Tel.: +36 702988539, +36 13922222x1732; fax: +36 13922215.
E-mail address: banyasz@sunserv.kfki.hu (I. Bányász).

0030-4018/$ - see front matter © 2008 Elsevier B.V. All rights reserved.
doi:10.1016/j.optcom.2008.04.075

and his co-workers [12,13]. In those experiments the highest spatial frequency of the implanted gratings was 250 lp/mm. Semiphysically developed phase holograms in Agfa 8E75HD emulsion were also studied by him using phase- contrast microscopy [14]. It was proved that phase-contrast microscopy could be used for the quantitative determination of the refractive index modulation in holographic phase gratings [15,16]. The above results made us hope that these standard microscopic techniques of phase object visualization could be suitable for studying high spatial frequency photorefractive gratings, too.

2. Experimental

2.1. Recording the holograms

For the investigation, we used an iron doped as grown lithium niobate sample. The crystal was grown by the Czochralski method with iron content of 10^{-3} molar ratio in the melt, using suprapur lithium carbonate (from Merck) and grade LN Nb_2O_5 materials (from H.C. Starck). The dimensions of the sample were $5 \times 0.3 \times 4\ mm^3$ in order of the crystallographic axes *a*, *b* and *c*, where *c* is the polar axis. The edges of the sample were short-circuited by silver paste. For recording the grating, we used standard two-wave mixing set-up with extraordinarily (horizontally) polarized recording beams, and with different angles of incidence. The set-up was similar than we used for thermal fixing experiments [17] or to investigate the effect of thermal neutron absorption to the decay of the photorefractive grating in $LiNbO_3$:Fe [18]. The wavelength of the recording beams was 488.0 nm, produced by an argon ion laser and a space filtering beam expander. The input intensities were adjusted using gray filters. We used an expanded and space-filtered laser beam of a He–Ne laser as a reading beam with intensity less than 0.01 mW/cm^2. The reading beam was adjusted into the Bragg angle of the grating using precision rotary and translating stage. The sample holder was mounted on a computer controlled precision rotary stage. After each microscopic measurement, we checked the diffraction efficiency by optimising the position of the rotary stage, reading beam and photodiodes both at the transmitted and the refracted beams. The signal of the photodiodes was measured using lock-in technique, and the sensitivity was increased by applying interference filters for 632.8 nm (Fig. 1).

In order to monitor the right value of the diffraction efficiency during recording, before each recording we recorded a new grating only for fine adjustments of the set-up. After the fine adjustment, we erased the grating by a fibre-optic 150 W tungsten halogen lamp for 20 min, and waited for at least 8 min for thermal equilibrium of the sample and the sample holder. After recording, we checked once again the diffraction efficiency by rotating the stage.

2.2. Microscopic study of the holograms

After terminating holographic recording, the photorefractive crystal was taken to the microscopy laboratory, and microphotographs of the holographic gratings were taken with a **Zeiss Peraval** microscope. That microscope can be used both as an interference- and a phase-contrast one, and there is a third option, the so-called interference phase-contrast (interphako), where optical path differences throughout the phase microobjects show up in different interference colours. After having checked all three methods, we opted for using interference microscopy. Phase-contrast microscopy (using high-power microscope objective) can resolve fine holographic gratings recorded in thick photorefractive crystals. However, in case of the routinely used thick (of some mm) samples, precise orientation of the sample with respect to the microscopic illumination becomes crucial. Small angular maladjustments can result in reduced phase-contrast. Furthermore, one has to take into account all the factors reducing the real phase-contrast, namely: modulation transfer function (MTF) of the microscope objective and that of each element (e.g. CCD camera) of the recording set-up. That is why we finally chose interference microscopy for the present experiments. In interference microscopy optical path differences are visualised as deformations of an equidistant parallel interference fringe system, consequently interference photomicrographs are much less susceptible to changes caused by the recording system.

2.3. Results of diffraction efficiency measurements

Recording and study of six series of holograms, in the same $LiNbO_3$:Fe sample, are presented in this article. Holograms of three

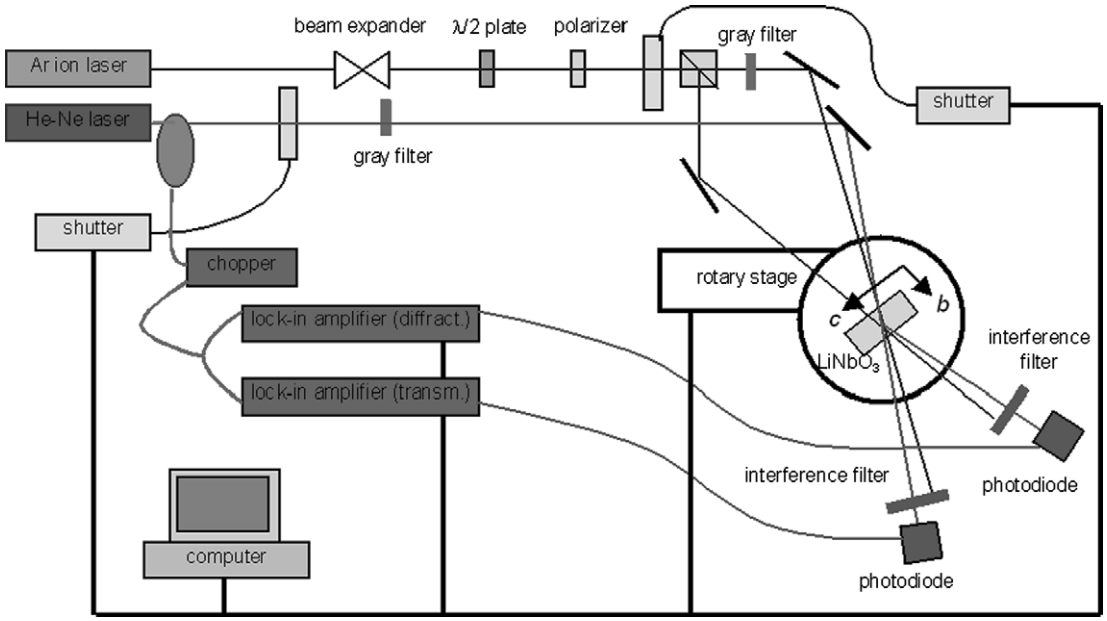

Fig. 1. The set-up for hologram recording in a photorefractive crystal.

Table 1
Grating constants (Λ) and recording fringe visibilities (V) for the six series of holograms

Number of series	Λ (μm)	V	Recording intensity I_0 (mW/cm^2)
1	3.0	0.530	48.1
2	3.0	1.000	44.0
3	6.5	0.527	47.8
4	6.5	0.997	47.8
5	8.8	0.530	48.0
6	8.8	1.000	48.1

values of grating constant (Λ) were recorded. Experiments were carried out at two values of recording interference fringe visibility (V) for each grating constant. These values are shown in Table 1. Bias intensity of the recording interference pattern was set around $I_0 = 50$ mW/cm^2 for all the series, its values are also indicated in the table.

Visibility of the recording interference fringes is defined as follows:

$$V = 2\sqrt{R}/(R+1) \tag{1}$$

where R is the intensity ratio of the interfering beams.

Diffraction efficiency of the photorefractive holograms measured at $\lambda = 632.8$ nm, as function of the recording bias exposure at $\lambda = 488.0$ nm, $E_0 = I_0\, t$, is presented in Figs. 2–4.

Build-up of holographic grating of a grating constant of $\Lambda = 3.0$ μm, at two values of the modulation of the recording interference fringes is shown in Fig. 2. In the first curve, although complete saturation was not attained, a saturation diffraction efficiency of about 1.1% can be extrapolated. Saturation could not be achieved at $V = 1.00$, either, due to a possible electric discharge caused by high local electric field. The highest diffraction efficiency was about 2.6%.

At $\Lambda = 6.5$ μm, saturation diffraction efficiency is 1.4% at $V = 0.530$, while recording at maximum fringe visibility results in a saturation diffraction efficiency of about 3.5% (Fig. 3.). However, the two curves show that the half values of saturation diffraction efficiency, $\eta_{sat}/2$ is attained at the same exposure, between 4500 and 5000 mJ/cm^2.

Difference in saturation diffraction efficiencies for the two visibilities is even higher for the holograms of the largest ($\Lambda = 8.8$ μm) grating constant. In the case of $V = 0.530$ $\eta_{sat} = 0.37\%$ and in the case of $V = 1.000$ $\eta_{sat} = 2.4\%$ (Fig. 4.).

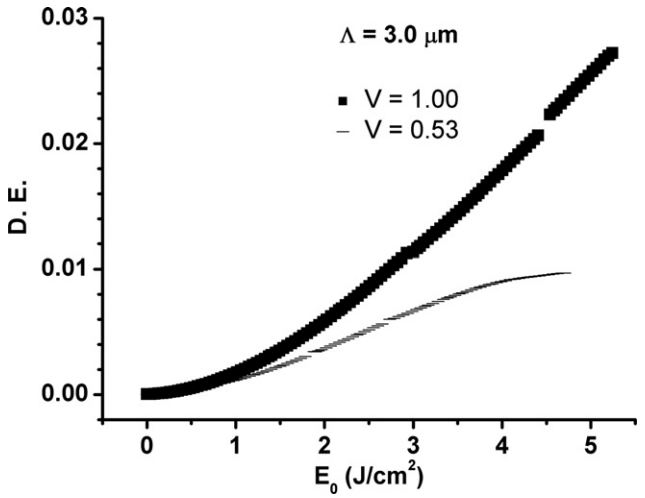

Fig. 2. Hologram build-up at $\Lambda = 3.0$ μm; $V = 0.530$ and 1.000. Recording intensity $I_0 = 48.1$ mW/cm^2.

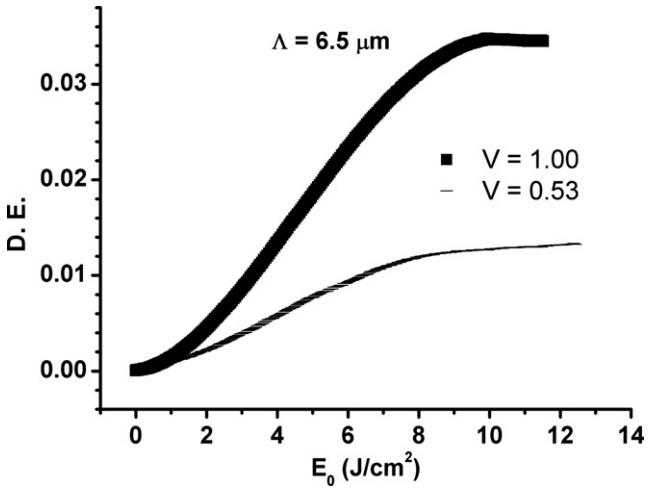

Fig. 3. Hologram build-up at $\Lambda = 6.5$ μm; $V = 0.527$ and 0.997. Recording intensity $I_0 = 48.0$ and 54.4 mW/cm^2, respectively.

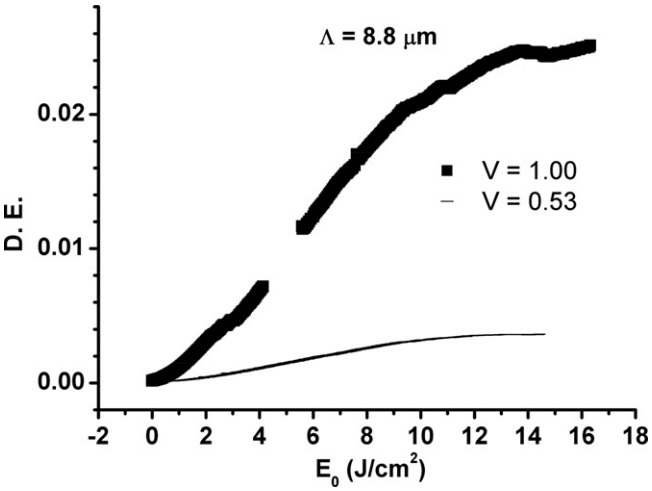

Fig. 4. Hologram build-up at $\Lambda = 8.8$ μm; $V = 0.530$ and $V = 1.000$. Recording intensity $I_0 = 48.1$ and 48.0 mW/cm^2, respectively.

2.4. Determination of the amplitude of refractive index modulation of the holograms

Inferring optical path differences from an interference microscopic image is straightforward. If we denote the wavelength of the monochromatic microscopic illumination with λ, the separation of two interference fringes in the microscopic image with D and the amplitude of the deformation of the interference fringe with y, we obtain the optical path difference Δs using the following formula:

$$\Delta s = \frac{y\lambda}{D} \tag{2}$$

If the phase object of thickness d is homogeneous in the direction of the microscopic illumination (z), the refractive index modulation will be:

$$\Delta n = \frac{\Delta s}{d} \tag{3}$$

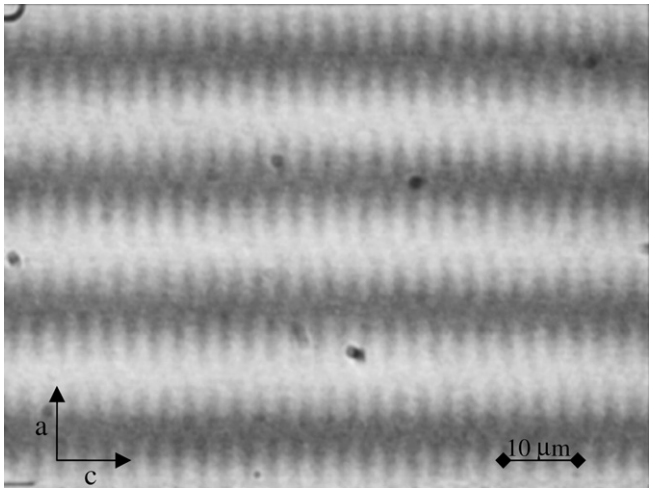

Fig. 5. Microinterferogram of a photorefractive hologram. $\Lambda = 3.0$ μm, first series, $V = 1.00$, Recording bias exposure at $\lambda = 488.0$ nm, $E_0 = 3960$ mJ/cm^2.

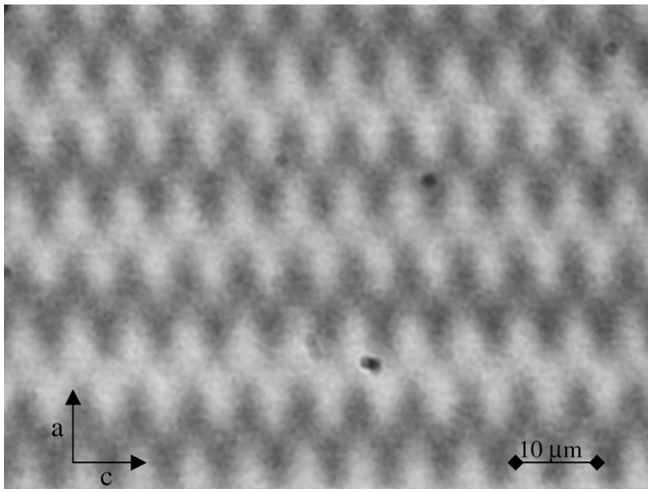

Fig. 6. Microinterferogram of a photorefractive hologram. $\Lambda = 6.5$ μm, third series, $V = 0.997$, Recording bias exposure at $\lambda = 488.0$ nm, $E_0 = 6528$ mJ/cm^2.

Three interference microscopic photomicrographs of holographic gratings recorded in the $LiNbO_3$ crystal are shown in Figs. 5–7. Orientation of the crystal axes and length scales are indicated in the figures.

A total of 45 microinterferogram has been recorded, 6–8 ones for each series. The available highest power dry microscope objective of 63X was used, with a 15X ocular and monochromatic illumination through a green interference filter (GIF), centred at $\lambda = 551$ nm, and grating ($C = 32$), to assure high-contrast interference fringes. We decided not to use the 100X (N.A.) immersion objective because it would have made sample handling more difficult and diffraction efficiency control less reliable.

Regular, quasi – sinusoidal grating profiles can be seen in each of the three figures. Although visibility of the interference fringes varied from one measurement to other, amplitude of the phase modulation of the fringes reproduced well when two microscopic measurements of the same hologram were done.

Interference microscopic photographs were contrast enhanced, and optical path variations were extracted from them. Extracting optical path variations from the microinterferograms is a straightforward but complicated task. Basically, it consists in the determination of the following values: 1. period of the unperturbed interference fringe system, seen in the microscope when no object is present 2. amplitude of the modulation of this fringe system due to the optical path changes across the holographic grating.

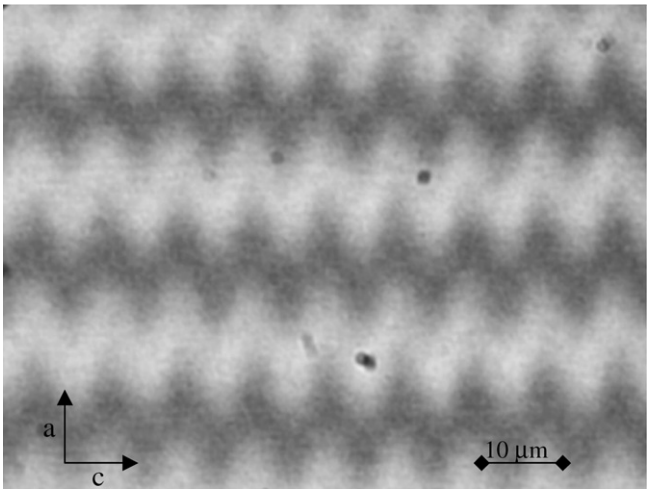

Fig. 7. Microinterferogram of a photorefractive hologram. $\Lambda = 8.8$ μm, fifth series, $V = 1.00$, Recording bias exposure at $\lambda = 488.0$ nm, $E_0 = 8640$ mJ/cm^2.

We used two methods to accomplish this task. The first one was a Matlab script, written for that purpose. We took profiles of the interferogram perpendicularly to the fringes exactly at the positions of the maxima and minima of the modulation of the fringes. Then location of the maxima and minima was determined by fitting an analytical function to the profiles. Then modulation can be obtained easily, knowing the wavelength used for the observation.

The second method differs from the first one only in the user interface and the functions and processes used to obtain the above-mentioned profiles. We used the FRIINT (fringe integrator) code [19,20]. It was developed by the Holography Group of the Department of Physics of Budapest University of Technology. The code fits a cosine function to the fringe profile, using an algorithm based on Fourier transformation.

We checked the two methods with various interferograms, and obtained the same values for the refractive index modulations. The results presented in this article have been obtained using the FRIINT code because it provides good visual control of the evaluation process. Note that the fitted cosine function practically coincides with the measured profile. This was the case for the majority of the interferograms, even for those of very low visibility, down to 0.10. Amplitude of the (quasi sinusoidal) refractive index modulation as a function of bias exposure for all the six series of holograms is presented in Figs. 8–10. The estimated random error of the refractive index modulation measurement is less than 2×10^{-5} (1×10^{-5} in average). Additional systematic error can occur in the range of $1 \cdots 2 \times 10^{-5}$ due to maladjustment of the microscope and the inhomogeneity of the grating.

The Δn (E_0) curves show an exponential saturation. According to the Kogelnik equation [21], in case of sinusoidal volume holographic gratings, diffraction efficiency is proportional to the squared sine of the refractive index modulation. Deviations from this rule in the above results can be attributed to the following facts: There occur fluctuations in the output power of the Ar ion laser, introducing uncertainty in the exposure. Microscopic illumination can also partially erase the photorefractive hologram, especially because we had to use a green interference filter to allow precise adjustment of the microscopic image of very low intensity. Finally, the photorefractive gratings themselves can have non-sinusoidal refractive index modulation.

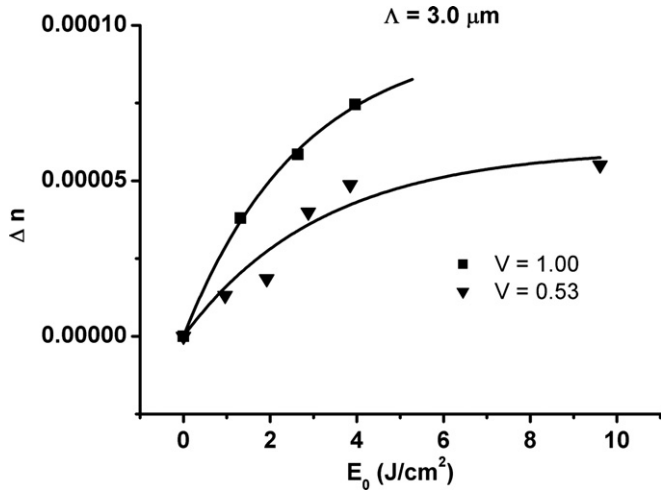

Fig. 8. Δn as a function of bias exposure. First and second series, $\Lambda = 3.0$ μm, $V = 0.530$ and 1.000.

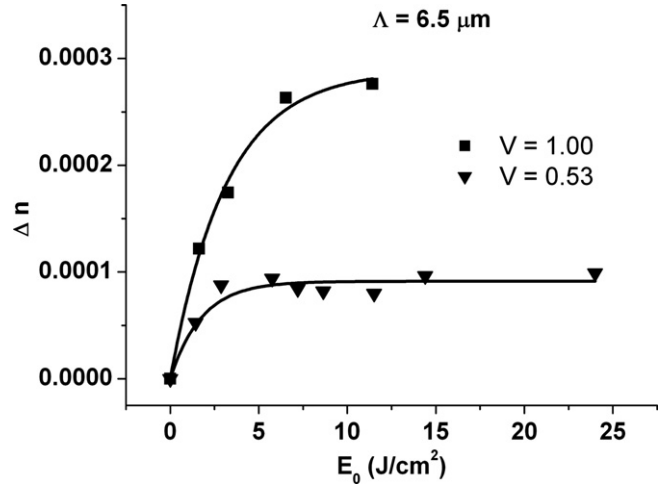

Fig. 9. Δn as a function of bias exposure. Third and fourth series, $\Lambda = 6.5$ μm, $V = 0.527$ and 0.997.

3. Conclusion

We adapted a classical method, interference microscopy to quasi in-situ observation of hologram build-up in photorefractive crystals. We demonstrated that fine holographic gratings ($\Lambda = 3.0$ μm) could be clearly visualized by this method. We performed quantitative analysis of the microinterferograms and determined amplitude of the refractive index modulation as a function of bias exposure (exposure time) for the build-up holographic grating of grating constants of $\Lambda = 3.0$, 6.5 and 8.8 μm in $LiNbO_3$:Fe crystal.

Besides of improving the present method, and applying it to the study of other photorefractive materials, development of a really in-situ (or real-time) set-up is also planned, using either classical or digital holographic interferometry, and special (long working distance) microscopy.

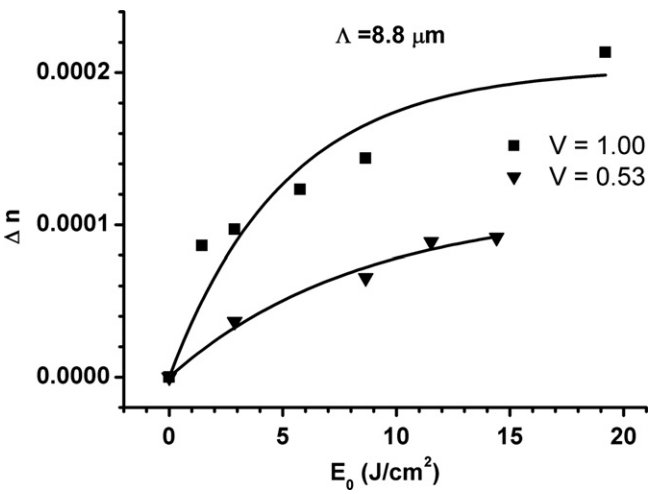

Fig. 10. Δn as a function of bias exposure. Fifth and sixth series, $\Lambda = 8.8$ μm, $V = 0.530$ and 1.000.

Acknowledgment

The authors thank the Holography Group, Department of Physics of Budapest University of Technology for providing them the FRIINT (fringe integrator) computer code. This research was funded by the Hungarian National Research Fund under grant No. T 047265.

References

[1] K. Buse, E. Krätzig, in: H.J. Coufal, D. Psaltis, G.T. Sincerbox (Eds.), Holographic Data Storage, Springer, Berlin, 2000, p. 113.
[2] R. Matull, R.A. Rupp, J. Phys. D: Appl. Phys. 21 (1988) 1556.
[3] R.A. Rupp, Appl. Phys. A 55 (1992) 2.
[4] P.S. Brody, C.G. Garvin, Ferroelectrics 107 (1990) 9.
[5] B. Poumellec, I. Riant, P. Niay, P. Bernage, J.F. Bayon, Optical Materials 4 (1995) 404.
[6] A.A. Grabar, A.I. Bercha, I.M. Stoika, Tech. Phys. Lett. (1–2) (1996) 22.
[7] M. Douay, W.X. Xie, P. Bernage, P. Niay, B. Boulard, Y. Gao, C. Jacoboni, H. Poignant, Proc. SPIE 2998 (1997) 58.
[8] G. Cipparrone, A. Mazzulla, F.P. Nicoletta, L. Lucchetti, F. Simoni, Opt. Commun. 150 (1998) 297.
[9] E. Soergel, W. Krieger, V.I. Vlad, J. Opt. Soc. Am. B 15 (1998) 2185.
[10] J.L. Zhao, P. Zhang, J.B. Zhou, D.X. Yang, D.S. Yang, E.P. Li, Chinese Phys. Lett. 20 (2003) 1748.
[11] M. de Angelis, S. De Nicola, A. Finizio, G. Pierattini, P. Ferraro, S. Pelli, G. Righini, S. Sebastiani, Appl. Phys. Lett. 88 (2006) 111114.
[12] I. Bányász, M. Fried, Cs. Dücsõ, Cs. Hajdú, Z. Vértesy, Proc. SPIE 1394 (1998) 120.
[13] I. Bányász, M. Fried, Cs. Dücsõ, Z. Vértesy, Appl. Phys. Lett. 79 (2001) 3755.
[14] I. Bányász, Opt. Commun. 192 (2001) 27.
[15] I. Bányász, Opt. Commun. 225 (2003) 269.
[16] I. Bányász, Appl. Phys. Lett. 83 (2003) 4282.
[17] M.A. Ellabban, G. Mandula, M. Fally, R.A. Rupp, L. Kovács, Appl. Phys. Lett. 78 (2001) 844.
[18] G. Mandula, R.A. Rupp, M. Balaskó, L. Kovács, Appl. Phys. Lett. 86 (2005). 141107/1-3.
[19] F. Gyímesi, V. Borbély, Sz. Mike, B. Ráczkevi, Z. Füzessy, Beyond the upper limit of holographic interferometry by scanning, in: Z. Füzessy, Gy. Ákos (Eds.), Denis Gabor Commemorative Conference: Symposium on Holography, Budapest, Hungary, June 2000, Conference CD, 2000.
[20] F. Gyímesi, V. Borbély, B. Ráczkevi, Z. Füzessy, J. Holography Speckle 1 (2004) 39.
[21] H. Kogelnik, The Bell Syst. Tech. J. 48 (1969) 2909.